frontiers | Frontiers in Molecular Biosciences

TYPE Methods
PUBLISHED 19 October 2022
DOI 10.3389/fmolb.2022.1004746

OPEN ACCESS

EDITED BY
Elsa Zacco,
Italian Institute of Technology (IIT), Italy

REVIEWED BY
Clément Charenton,
INSERM U964 Institut de Génétique et de Biologie Moléculaire et Cellulaire (IGBMC), France
Azzurra Codino,
Italian Institute of Technology (IIT), Italy

*CORRESPONDENCE
Monica Ballarino,
monica.ballarino@uniroma1.it

†These authors contributed equally to this work and share first authorship

SPECIALTY SECTION
This article was submitted to RNA Networks and Biology, a section of the journal Frontiers in Molecular Biosciences

RECEIVED 27 July 2022
ACCEPTED 30 August 2022
PUBLISHED 19 October 2022

CITATION
Desideri F, D'Ambra E, Laneve P and Ballarino M (2022), Advances in endogenous RNA pull-down: A straightforward dextran sulfate-based method enhancing RNA recovery. *Front. Mol. Biosci.* 9:1004746. doi: 10.3389/fmolb.2022.1004746

Advances in endogenous RNA pull-down: A straightforward dextran sulfate-based method enhancing RNA recovery

Fabio Desideri[1†], Eleonora D'Ambra[1†], Pietro Laneve[2] and Monica Ballarino[3*]

[1]Center for Life Nano- & Neuro-Science of Istituto Italiano di Tecnologia (IIT), Rome, Italy, [2]Institute of Molecular Biology and Pathology, National Research Council, Rome, Italy, [3]Department of Biology and Biotechnologies "Charles Darwin", Sapienza University of Rome, Rome, Italy

Detecting RNA/RNA interactions in the context of a given cellular system is crucial to gain insights into the molecular mechanisms that stand beneath each specific RNA molecule. When it comes to non-protein coding RNA (ncRNAs), and especially to long noncoding RNAs (lncRNAs), the reliability of the RNA purification is dramatically dependent on their abundance. Exogenous methods, in which lncRNAs are *in vitro* transcribed and incubated with protein extracts or overexpressed by cell transfection, have been extensively used to overcome the problem of abundance. However, although useful to study the contribution of single RNA sub-modules to RNA/protein interactions, these exogenous practices might fail in revealing biologically meaningful contacts occurring *in vivo* and risk to generate non-physiological artifacts. Therefore, endogenous methods must be preferred, especially for the initial identification of partners specifically interacting with elected RNAs. Here, we apply an endogenous RNA pull-down to lncMN2-203, a neuron-specific lncRNA contributing to the robustness of motor neurons specification, through the interaction with miRNA-466i-5p. We show that both the yield of lncMN2-203 recovery and the specificity of its interaction with the miRNA dramatically increase in the presence of Dextran Sulfate Sodium (DSS) salt. This new set-up may represent a powerful means for improving the study of RNA-RNA interactions of biological significance, especially for those lncRNAs whose role as microRNA (miRNA) sponges or regulators of mRNA stability was demonstrated.

KEYWORDS

RNA pull-down, RNA/RNA interactions, lncRNA, microRNA, Dextran sulfate sodium salt

Introduction

Since the first characterization of RNA, DNA and protein chemical composition, it has becoming increasingly clear the need to carve the interactions that these macromolecules establish in living cells to execute their functions (Matthews, 1988; Moore, 2005). On this line, protein-centric methodologies for the antibody-mediated detection of specific peptide/nucleic acid contacts (Phizicky and Fields 1995), have greatly impacted molecular biology research. Along with the discovery of several classes of non-protein-coding RNAs, the need to study their functions prompt to develop increasingly refined technologies for characterizing their physical association with individual proteins (as reviewed in Cipriano and Ballarino, 2018). The native RNA immunoprecipitation (RIP) (Lerner and Steitz 1979) represented the first method developed for this purpose, which was followed in the early 2000s by the development of UV-crosslinking and immunoprecipitation (CLIP) assays and subsequent CLIP-based methods (Ule et al., 2003; Lee and Ule 2018; Hafner et al., 2021). Over the years these approaches were gradually flanked by the development of complementary RNA-centric methods, in which the putative interactors of a given RNA are specifically purified by using antisense DNA probes as baits (McHugh et al., 2015; Ramanathan et al., 2019).

Among the RNA-centric approaches, the methodologies allowing to detect RNA/RNA contacts train great attention, also in light of the ever-increasing importance of base-complementarity between transcripts, both in a mechanistic and in a regulative perspective (Helwak et al., 2013; Engreitz et al., 2014; Guil and Esteller, 2015). Although these strategies already contribute in a significant manner to functional/descriptive studies of RNA-RNA and protein interactions, continuous adjustments are required to adapt the experimental protocols to specific case studies. The latter observation largely applies to long noncoding RNAs (lncRNAs) which, especially in the last three decades, have been shown to greatly contribute to regulate gene expression in the nucleus and cytoplasm (Li and Chang, 2014; Herman et al., 2022). Consequently, aberrant lncRNA expression has been implicated in a variety of human diseases, including cancer, cardiovascular and neurological disorders (Fatima et al., 2015; Lekka and Hall, 2018; Ni et al., 2022).

LncRNAs represent an heterogenous class of non-protein coding molecules arbitrarily defined as transcripts longer than 200 nucleotides, which regulate gene expression through transcriptional as well as post-transcriptional mechanisms (Yao et al., 2019; Statello et al., 2021). Many of them are not constitutively active but exert regulatory roles, which makes their study particularly challenging. In fact, their low abundance at the steady-state level, their restricted expression to specific cell subtypes or developmental windows and their modest evolutionary conservation, often makes the lncRNA-mediated gene regulation extremely circumscribed and hard-to-be unraveled (Fatica and Bozzoni 2014; Kopp and Mendell, 2018).

From a mechanistic standpoint, lncRNAs function through the interaction with other biomolecules (Ferrè et al., 2016), and several examples suggest a crucial role for local lncRNA-RNA contacts at the root of their activities (Gong and Maquat, 2011; Carrieri et al., 2012; Kretz et al., 2013; Martone et al., 2020). Overall, these observations suggest that practices which aim to ameliorate the identification of bound partners from complex cellular extracts represent a critical step to clarify noncoding RNA-mediated cellular activities. Several databases and *in silico* tools were developed for the prediction of lncRNA functions based on lncRNA-RNA interactions (Bellucci et al., 2011; Fukunaga, and Hamada, 2017; Gong et al., 2018; Fukunaga et al., 2019). In parallel, experimental procedures have evolved to globally enhance the reliability and efficacy in detecting RNA-RNA interplays (Cai et al., 2020).

Hereinafter, we propose a strategy which represents a variation on the theme of the standard RNA pull-down (PD), with the innovative use of the Dextran Sulphate Sodium (DSS) salt as a hygroscopic chemical additive. By testing the procedure to the motoneuron-expressed lncRNA lncMN2-203 (Biscarini et al., 2018; Carvelli et al., 2022), we found that DSS 1) greatly improves the purification of lncMN2-203, as compared to previous analysis and, importantly, 2) facilitates the identification of its RNA binding partner, the microRNA miRNA-466i-5p. These results promise to upgrade RNA functional analyses in a straightforward and effective manner.

Materials and equipment

Oligonucleotide probe design and sequences

A number of 15 oligonucleotide probes, 90-nucleotides long and carrying a 5'-biotin modification, were designed as in McHugh et al., 2015 to cover the lncMN2-203 sequence. U1 snRNA Probes (Desideri et al., 2020) were used as a control.

Buffer composition

Lysis buffer

Tris-HCl pH 7.5 50 mM, NaCl 150 mM, MgCl2 3 mM, NP40 0.5%, EDTA 2 mM. Add fresh DTT 1 mM, 1× PIC, and RNase Inhibitors (0.2 U/µl).

Hybridization buffer (HB)

Tris-HCl pH 7.5 100 mM, NaCl 300 mM, MgCl2 1 mM, SDS 0.2%, Formamide 15%, NP40 0.5%, EDTA 10 mM. Add fresh DTT 1 mM, 1× PIC, and RNase inhibitors (0.2 U/µl).

TABLE 1 List of biotinylated probes used for LncMN2 RNA Pull down.

LncMN2. PD1	AACTTCTGGCCATTTTCAACCCATTTGCTCCAGTTCACAGCACTCACGCAGAAGTATGGCACTGAGGGGCT CAG GATACCTCAGGAATGA
LncMN2. PD2	ATCTTCCTGGATTTACCGACCTCAGGCTCCAGTTCTGCATAATTAGCTTAAACTGGCTCAAATGGATTTTAACTG GTCAGAAATTCAATT
LncMN2. PD3	TCTTGGAGCCTTGGTTTTCTCATCATATCACAAAGCCTCCAGTCACCACAGGGCCAGGGTGAAGTCAAGGAAGAA GTGAAGCTGGAATCC
LncMN2. PD4	ACTCCGTGAAGGTGCTGGCTCTTAGGCCACTTAATAGCTGCATTCTAGGGAGCAGCAGGATAACAGGGAAACCAG AAGCTGATGACTGGC
LncMN2. PD5	AGAAGGCCTCCAACACAAGCATCAGCCTCCTTGAGACTATATAGATCACTATTGCTGTTAGTTCAAGCATTGGGA ATTTCCATAGGCTGA
LncMN2. PD6	AAGAATGATGGAGTTTCTGCTTTTATGGTTCATTCCTTGTGTACAGCAGAGGAAAAAGTGTTTATAAGGCCAGAT GGATATGGAAGATGC
LncMN2. PD7	TCATCCCAGAGCCAGCAGAACCCACTGGCTCAACTGCACAACAATTTTCAACAGTCCACATATTAAAGGGCTTTT CAACAATGTGGTTCT
LncMN2. PD8	CTATACATCAGCTACAATCATGTACTGGCACTGGGCTAAAGACCATGTGACTTTATCTTCCTTCAATATGGTATT AATTTTCACCAAGAA
LncMN2. PD9	GCCCAGGCAGAGTTGGATGGTGGAGGAAGTCCACAACCCTAGCCTAAAAAGCAGTGTGCTAGTGGTGCAGATCAA CTCTACATTCCTATC
LncMN2. PD10	TGATCCCTTTCTTATGGTGAGCTCAGTCCTCTGAGGACTTCTGTTGTTGCTGTTAATTAAGACTGACATAAGGAG ACAAGCAGACATTGA
LncMN2. PD11	TTATGTGTGACTGTGTGTCCCACACTCAGTGAGTAACTTTGAACCAAGGATAAGAATTGAGTTGGAGCCTAGGAC TTGGGGAAGAAGGCT
LncMN2. PD12	TAAATATAAACATCCACATTAAAATCACCTTAGTCAGCTATGAGTGAAGAATATGTATCCTACACAGTTCTTTGC TAGATATTTTAGCTC
LncMN2. PD13	CCCTCCCAGAATGATCAACAGATCCTGTATTATAAGTTCTAAGAGTGTCTACTTTTGCAACAGCTCTGATCCATT TGTGGTCATAGTCAT
LncMN2. PD14	CTCAGTTGGGACCCAATGATGTTAACCTTAGTCTTGTGCTTGTTGTATTTCTCCACTATGAGCTGACTTTGCCTCTTA TTCTGGACTCCA
LncMN2. PD15	AGATAGAGATCCGTTTTTCTCTTCTTCTCCATCATTTTACCATGTTTTTTCCATTGTCTTTAAACTTGAAGCAGAATC TTTATTTTAATG

Reagent list

1) Streptavidin Magnesphere paramagnetic beads—Promega.
2) Dextran Sulfate Sodium (DSS) salt—SigmaAldrich
3) cOmplete™, Mini, EDTA-free Protease Inhibitor Cocktail (PIC)—ROCHE.
4) RNase Inhibitor: RiboLock—ThermoFisher Scientific.
5) Tris, NaCl, MgCl2, SDS, Formamide, NP40, EDTA and Dithiothreitol (DTT)—SigmaAldrich.
6) TRI-Reagent—Zymo Research.
7) Direct-zol RNA Miniprep Kit and DNase—Zymo Research.
8) Superscript VILO™ cDNA Synthesis Kit—ThermoFisher Scientific.
9) SYBR Green Power-UP - ThermoFisher Scientific
10) miScript II RT Kit—QIAGEN
11) miScript SYBR Green—QIAGEN.

Experimental procedure

mESCs carrying the Hb9:GFP transgene (Wichterle et al., 2002) are differentiated to motoneurogenesis through embryoid bodies (EB) formation as previously described (Wichterle and Peljto, 2008). Embryoid bodies at day 6 of differentiation (EB6) are harvested in PBS and centrifuged at 400 x g for 5 min, before proceeding as follows:

1) Gently resuspend cell pellets from EB6 in lysis buffer supplemented with proteases (1X PIC- ROCHE) and RNase inhibitors (0.2 U/µl—Thermo Fisher Scientific). Live, freshly isolated, not frozen cells should be preferred.
2) Incubate the cell suspension first on ice (10 min) and then on a rotating wheel for 10 min at 4°C. Centrifuge the cell suspension at 15,000 × g at 4°C for 15 min and collect the supernatant, which represents the total cellular extract, into new tubes. Quantify the extract by protein determination and dilute 1:2 in Hybridization Buffer (HB). From the diluted extracts, collect 1 mg of material for each PD condition and 0.1 mg for the Input (i.e., 10% of the PD sample). Typically, 10 millions of freshly lysed EB6 yield up to 1 mg of total extract. CRITICAL STEP: since DSS can interfere with enzymatic reactions, collect Input before DSS addition to the EB6 total extract or use

specific RNA purification methods to remove possible salt contaminants. A final volume of 0.9 ml in a 1.5 ml vial tube is the ideal condition for hybridization.

3) Add DSS salt (SigmaAldrich) to each PD sample at a final concentration of 1% or 2.5%. CRITICAL STEP: DSS can be very viscous when undiluted, be careful to pipette the required volume. Cutting the tip of the pipette could help.
4) Dilute 100 pmol of 5′-biotinylated (90-mer long) antisense DNA oligonucleotide probes specifically targeting lnc-MN2 or U1snRNA to a final volume of 50 µL with HB. Heat-denature the probes for 3 min at 80°C and directly add to each sample (MN2 PD, U1 PD).
5) Mix the specific probes with the cellular extract and incubate at 4°C for, at least, 4 h. Incubate Input and PD samples in parallel. Before concluding the incubation, gently wash 0.1 ml of Streptavidin paramagnetic beads (Promega)/sample with HB on a magnetic rack (Millipore). Repeat this step. CRITICAL STEP: prior to pipette the needed amount of beads, gently flick the bottom of the tube until the particles are completely dispersed.
6) Resuspend the Streptavidin paramagnetic beads in 0.1 ml of fresh HB and then add to each PD sample.
7) Incubate beads/extract/probe for 1 h at RT (20–25°C). On a magnetic rack, remove the supernatant from the beads and discard as it contains the unbound material. Keep the beads for steps 8–9!
8) Carefully wash the beads 4 times (3 min each) on a rotating wheel with HB at RT (20–25°C). After each wash, recover the beads on a magnetic rack.
9) For RNA extraction, add Trizol (TRI Reagent- Zymo Research) directly on the washed beads and vortex thoroughly for 2 min to detach the probes. Place back the samples on the magnetic rack and collect the supernatant in a new 1.5 ml tube. CRITICAL STEP: the supernatant contains RNA. Keep it for RNA extraction!
10) Purify the RNA with Direct-zol RNA Miniprep Kit (Zymo Research), according to manufacturer's instructions and treat with DNase at RT (20–25°C). Elute RNA in 30 µL of Elution Buffer (Zymo Research) or DNase/RNase-Free Water. *OK to store RNA at −20°C at this point.
11) For long RNA transcript quantification, perform reverse transcription with SuperScript™ VILO™ cDNA Synthesis Kit (ThermoFisher Scientific), according to manufacturer's instructions and qRT-PCR with SYBR Green Power-UP (ThermoFisher Scientific). For miRNA quantification, perform reverse transcription with miScript II RT Kit (QIAGEN) and qRT-PCR with miScript SYBR Green (QIAGEN). 250–500 µg of RNA for each reverse transcription reaction is the ideal amount.

Results

The abovementioned protocol is thought to optimize the performance of the classical endogenous RNA PD procedures, with the aim to increase the recovery of the targeted lncRNA and, consequently, the specific enrichment of its co-precipitated RNA interactors.

The efficacy of the procedure was tested on lncMN2-203 (Figure 1A), a motor neuron (MN) specific lncRNA (Biscarini et al., 2018) recently found to control the specification of murine MNs by acting as a miRNA sponge (Carvelli et al., 2022). By using the same amount of total cell extract (2 mg of Input) previously used for lncMN2-203 precipitation (Carvelli et al., 2022), we reproduced its significant enrichment as compared to U1 snRNA PD, used as a control (Figure 1B). In accordance with the earlier analyses, the recovery of the other lncRNA isoforms (lncMN2-202/204) was almost null, in both the specific and control samples. In this setting, we also checked for miRNAs known to co-precipitate with lncMN2-203 and we confirmed that miR-466i-5p was significantly enriched in the MN2 as compared to the U1 PD (Figure 1C, left panel). MiR-669a-5p and miR-325-3p, used as negative controls, were almost undetectable in both the conditions (Figure 1C, middle and right panels), in line with their known inability to interact with the lncRNA (Carvelli et al., 2022).

Building upon these results, we wondered whether we could improve the cost-effectiveness of the procedure without reducing the performances. The evidence that lncRNA expression is often restricted to specific cell sub-populations causes not negligible concentration constrains (Goff et al., 2015). This is even more evident when the total cellular extracts are not prepared from FACS-sorted cells but rather from mixed cell populations, where the lncRNA average expression might be diluted. These aspects, that severely risk to impact the performance of the endogenous PD approaches, make lncMN2-203 as the most suitable candidate for testing the protocol. In fact, previously performed single-cell RNA-sequencing (scRNA-seq) showed that lncMN2-203 expression is restricted to a specific subpopulation of EB6 cells, namely the late MNs (Carvelli et al., 2022).

With the aim to reduce unnecessary costs, lncMN2-203 PD was repeated by halving the Input used in our original set-up (Figure 1A) to 1 mg of total lysate. Such a scale-down can be particularly useful when the targeted RNA is expressed in model systems whose maintenance and handling is costly and labor intensive. The mouse embryonic stem cells used for the characterization of lncMN2-203 perfectly fit in this example, as they require multiple passages for cell expansion and differentiation towards MNs, through the formation of EB (Figure 2A). In these new conditions, while the recovery of the lncRNA remained significant compared to the U1 control, the lncMN2-203 yield, calculated as percentage of Input, was about ten-fold lower than previously obtained (Figure 2B and

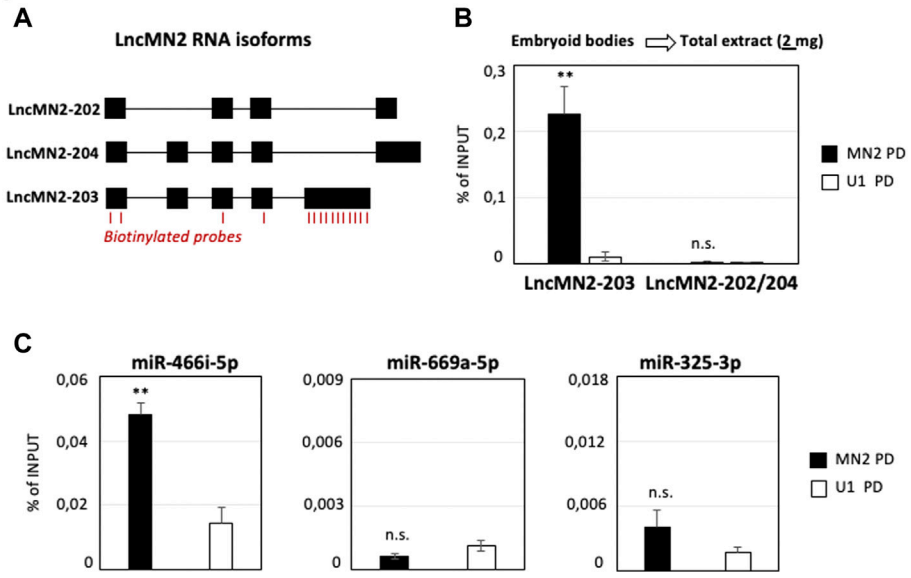

FIGURE 1
LncMN2-203 RNA pull-down in mESCs-derived embryoid bodies. **(A)** Block-and-line scheme representing the structure of the three lncMN2 RNA isoforms (Carvelli et al., 2022). Exon (black blocks)/intron (thin lines). The position of the antisense probes used for the RNA pull-down experiments is highlighted in red. **(B)** Quantification by qRT-PCR of lncMN2-203 and lncMN2-202/204 recoveries from lncMN2-203 (MN2) or control (U1 snRNA) RNA pull-down experiments. A total of 2 mg cell extracts prepared from differentiated EB6 were used for each reaction. LncRNA enrichments are expressed as Input percentage (%). Error bars represent SEM. n = 3 biological replicates. **(C)** Quantification by qRT-PCR of miR-466i-5p (Left), miR-669a-5p (Middle) and miR-325-3p (Right) recoveries from lncMN2-203 (MN2) or control (U1 snRNA) pull-down experiments. MiRNA enrichments are expressed as Input percentage (%). Error bars represent SEM. *n* = 3 biological replicates. Data information: $^{**}p \leq 0.01$, n. s.> 0.05 (two-tailed, unpaired Student's t-test).

Supplementary Figure S1A). More importantly, the diminished RNA recovery was not sufficient to co-precipitate the lncMN2-203 interactor, miRNA-466i-5p (Supplementary Figure 1A).

Exploring further resolutive options, we considered to use DSS salt, based on its well-known ability to accelerate probes-to-target hybridization (Lederman, et al., 1981), increasing fluorescent signals (Van Gijlswijk, et al., 1996) and reducing background (Singh and Jones, 1984). Together, these properties make the DSS particularly useful in RNA Fluorescence *In Situ* Hybridization (RNA-FISH) experiments for the visualization of both mRNA (Singer and Ward, 1982) and other transcripts which are less abundant, as with most lncRNAs (Ballarino et al., 2018; Santini et al., 2021). This feature is due to the chemical composition of this polysaccharide containing 17–20% sulfur that, being a highly water-soluble natural polymer, sequesters H2O molecules and enhances the effective concentration of DNA probes available for nucleic acid targeting (Figure 2C and Wetmur, 1975). Normally, the working concentration of DSS on membrane-immobilized or cell-fixed nucleic acids is ~10% of the final reaction volume (Wahl et al., 1979). At these concentrations of DSS, the solution appears viscous, and this could hamper the homogeneous mixing of RNA/protein extracts with the specific antisense oligonucleotide probes, which is crucial for the success of the PD assay. For this reason, the RNA PD was repeated by keeping constant the extract amount (1 mg), which was incubated with two different concentrations of DSS, specifically 1% and 2.5% of the final reaction volume (Figure 2C). Interestingly, in the two conditions we obtained a ~25 and ~280 -fold enrichment of lncMN2-203 respectively, measured as percentage of Input, as compared to the PD performed without DSS (DSS minus, Figure 2D and Supplementary Figure 1B). This dramatic enhancement in lncMN2-203 purification was accompanied by a slightly significant (but much lower respect to lncMN2-203) enrichment of the lncMN2-202/204 isoforms, as compared to the control (Figure 2D and Supplementary Figure 1B). This may be explained by the partial overlap between lncMN2-203 and lncMN2-202/204 sequence isoforms, together with the fact that a fraction (4 out of 15) of the capturing oligonucleotides targets the lncMN2 shared exons (Table 1).

Encouraged by these results, we then checked for lncMN2-203 miRNA interactors in the 1% and 2.5% DSS PD samples. Interestingly, we found that both the percentage and the specificity of miRNA purification responded to the efficiency of lncMN2-203 PD, as miR-466i-5p enrichment was significantly higher in the 2.5% than in the 1% DSS sample (Figure 2E and Supplementary Figure 1B). Importantly, in none of the two conditions any significant enrichment was found for the negative controls, the miRNAs miR-669a-5p and miR-325-3p, which is in line with the specificity of the antisense

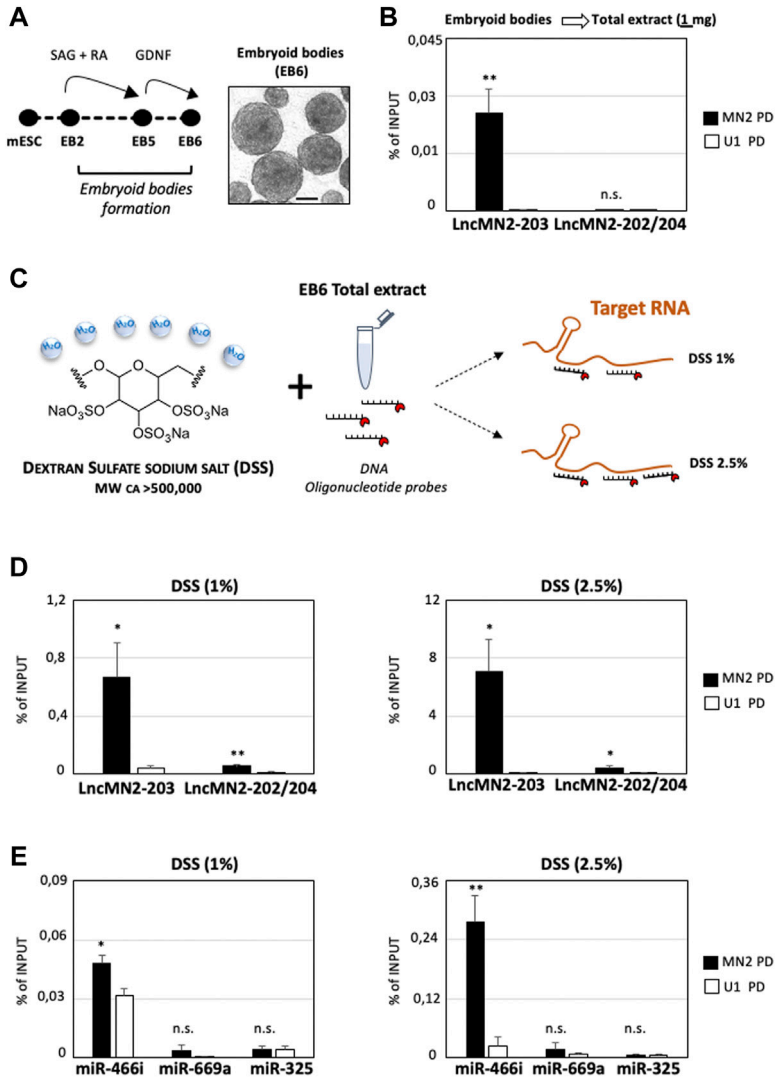

FIGURE 2
Dextran Sulfate Sodium salt increases the enrichment of LncMn2-203 and its miRNA interactor. **(A)** Left: Schematic representation of mESC-derived embryoid bodies differentiation (Capauto et al., 2018; D'Ambra et al., 2021). A representative field of EBs at day 6 of differentiation (EB6) is shown aside. Scale bar: 100 μm. SAG = Smoothened Agonist; RA = Retinoic Acid; GDNF = Glial cell line-derived neurotrophic factor. **(B)** Quantification by qRT-PCR of lncMN2-203 and lncMN2-202/204 recovery from lncMN2-203 (MN2) or control (U1 snRNA) pull-down experiments. A total of 1 mg of cell extracts prepared from differentiated EB6 were used for each reaction. LncRNA enrichments are expressed as Input percentage (%). Error bars represent SEM. *n* = 3 biological replicates. **(C)** Scheme of the Dextran Sulfate sodium salt (DSS) chemical structure and hygroscopic properties. By sequestering H20 molecules, the DSS salt increases the local concentration of DNA antisense probes targeting nucleic acid. **(D)** Quantification by qRT-PCR of lncMN2-203 and lncMN2-202/204 recoveries from lncMN2-203 (MN2) or control (U1 snRNA) RNA pull-down experiments. Different doses of DSS, 1% (Left) or 2.5% (Right), were used for each reaction. LncRNA enrichments are expressed as Input percentage (%). Error bars represent SEM. *n* = 3 biological replicates. **(E)** Quantification by qRT-PCR of miR-466i-5p, miR-669a-5p and miR-325-3p recoveries from lncMN2-203 (MN2) or control (U1 snRNA) RNA pull-down experiments. Different doses of DSS, 1% (Left) or 2.5% (Right), were used for each reaction. MiRNA enrichments are expressed as Input percentage (%). Error bars represent SEM. *n* = 3 biological replicates. Data information: $*p \leq 0.05$, $**p \leq 0.01$, n. s.> 0.05 (two-tailed, unpaired Student's t-test).

oligonucleotide probes, even in the presence of DSS (Figure 2E and Supplementary Figure 1B).

It was previously reported that DSS inhibits the activity of reverse transcriptase enzymes and the amplification by PCR (Kerr et al., 2012; Viennois et al., 2013; Juritsch and Moreau, 2019). However, the DSS-treated PD samples were normally PCR-amplified, likely because the repeated washing steps which precede the RNA extraction (see Experimental Procedure) remove any DSS residue potentially interfering with the RNA analysis. For these reasons, we recommend collecting the Input (EB6 total extracts) before adding DSS to the samples, or to use specific RNA purification methods to remove possible salt

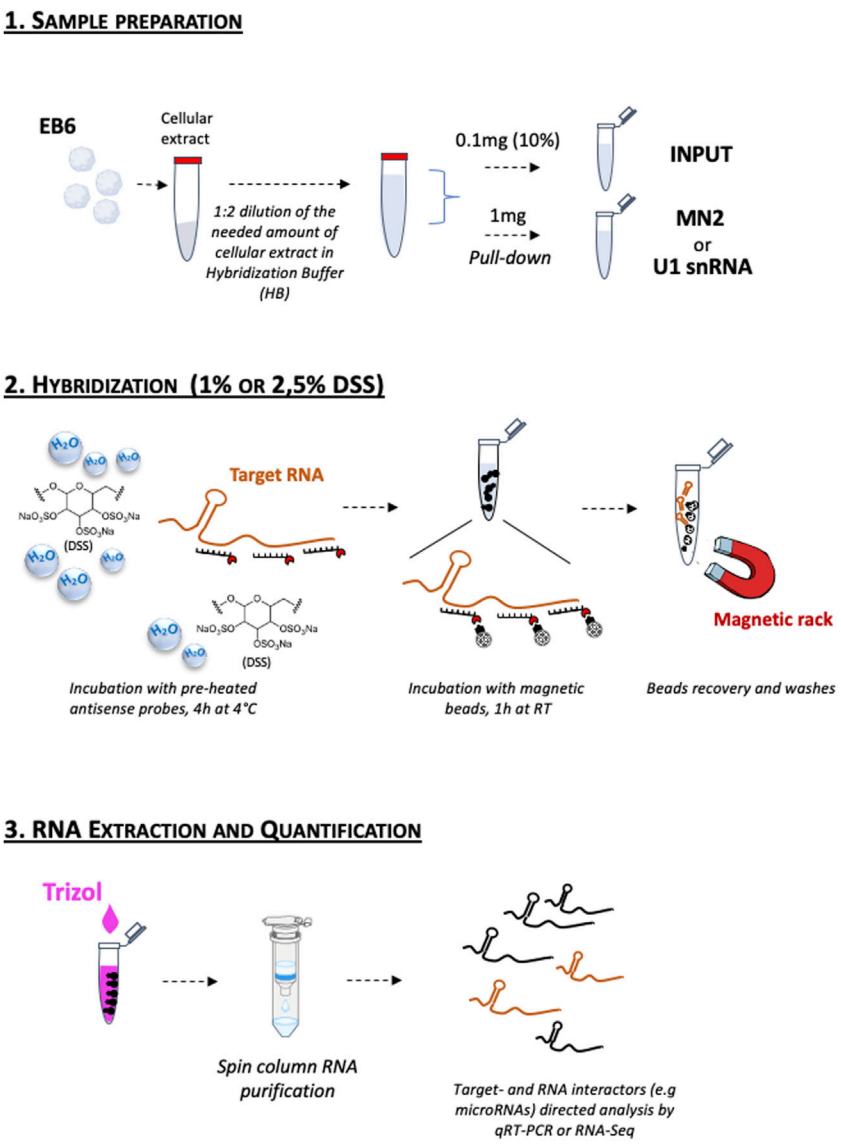

FIGURE 3
Schematic representation of the DSS-based RNA pull-down assay workflow. 1. Sample preparation; 2. Hybridization; 3. RNA Extraction and Quantification. The detailed protocol is reported in the Experimental Procedure section.

contaminants. All the experimental steps are schematized in Figure 3.

Concluding remarks

Here we provide a straightforward protocol, with comments and tips, which optimizes the classical endogenous RNA PD approach. We show that, at specific concentrations, the addition of DSS during precipitation dramatically increases the recovery of targeted RNAs without affecting their binding to the physiological partners. As an example, we tested the performance of the new set-up on lncMN2-203, whose isolation from 1 mg of DSS-treated extracts was found enhanced. Moreover, we found that the DSS treatment also improved the recovery of miR-466i-5p, previously identified as a functional lncMN2-203 partner (Carvelli et al., 2022). In line with the binding specificity, only background enrichments were found for miR-669a-5p and miR-325-3p, previously shown as non-interacting miRNAs.

Although the RNA PD experiments must be adapted to the specific abundance of the target RNA molecule in the suitable model system, we believe that the improvement here presented will be of great help for many scientists working across the field of

RNA biology and networks. Despite the proven effectiveness of the current protocols, the RNA purification still represents a technical challenge for the isolation of classes of transcripts, as lncRNAs, whose expression can be low or diluted across heterogeneous cell populations. This is also highlighted by the recent single cell (sc)RNA sequencing technologies showing that the expression of given RNAs can be extremely cell type specific, thus underrated in total extract, especially for those whose expression is further restricted to specific time and space windows (Savulescu et al., 2020).

Forthcoming perspectives

We have tested the feasibility and the outcomes of a new RNA precipitation protocol, by narrowing our attention to lncMN2-203, a lncRNA recently demonstrated to be functionally relevant through a mechanism of lncRNA/miRNA interaction. In principle, we cannot predict any technical restriction that may impede, in the future, downstream transcriptomics for a deeper and unbiased identification of the lncRNA-RNA interactome. Moreover, we believe that the improvements to the endogenous RNA PD protocol herein presented could also be applied to future studies on other RNA partners (e.g. proteins) or other RNA substrates. For instance, it may serve as a beneficial tool for the analysis of difficult-to-precipitate ncRNAs, such as circular RNAs (circRNAs), covalently closed lncRNAs generated by back-splicing of canonical pre-mRNAs (Kristensen et al., 2019). The mechanism of action of this class of transcripts often implies the association with other RNAs (Hansen et al., 2013; Piwecka et al., 2017), whose identification is hampered by the fact that the back-splicing junction is the only circRNA distinctive site, as compared to their linear precursors. Additional physical-chemical treatments of the cells (e.g., ultraviolet light or psoralen crosslinking) that have not been tested in the current study, can also be envisaged for the detection of more direct RNA-RNA interactions.

Data availability statement

The original contributions presented in the study are included in the article/Supplementary Material, further inquiries can be directed to the corresponding author.

Author contributions

FD and ED: Conceptualization, Methodology, Investigation, Validation, Writing-Original draft preparation. PL: Supervision, Validation, Writing- Reviewing and Editing. MB: Conceptualization, Writing-Reviewing and Editing, Funding acquisition.

Funding

This work was partially supported by the grants from: Sapienza University (prot. RM12117A5DE7A45B and RM11916B7A39DCE5) and POR FESR Lazio 2020-T0002E0001 to MB; CNR project NUTRAGE FOE-2021 DBA. AD005.225 to PL.

Acknowledgments

We thank Manuel Beltran for helpful discussion and advice on the experimental procedures.

Conflict of interest

The authors declare that the research was conducted in the absence of any commercial or financial relationships that could be construed as a potential conflict of interest.

Publisher's note

Supplementary material

The Supplementary Material for this article can be found online at: https://www.frontiersin.org/articles/10.3389/fmolb.2022.1004746/full#supplementary-material

References

Ballarino, M., Cipriano, A., Tita, R., Santini, T., Desideri, F., Morlando, M., et al. (2018). Deficiency in the nuclear long noncoding RNA Charme causes myogenic defects and heart remodeling in mice. *EMBO J.* 37 (18), e99697. doi:10.15252/embj.201899697

Bellucci, M., Agostini, F., Masin, M., and Tartaglia, G. G. (2011). Predicting protein associations with long noncoding RNAs. *Nat. Methods* 8 (6), 444–445. doi:10.1038/nmeth.1611

Biscarini, S., Capauto, D., Peruzzi, G., Lu, L., Colantoni, A., Santini, T., et al. (2018). Characterization of the lncRNA transcriptome in mESC-derived motor neurons: Implications for FUS-ALS. *Stem Cell Res.* 27, 172–179. doi:10.1016/j.scr.2018.01.037

Cai, Z., Cao, C., Ji, L., Ye, R., Wang, D., Xia, C., et al. (2020). RIC-seq for global *in situ* profiling of RNA-RNA spatial interactions. *Nature* 582 (7812), 432–437. doi:10.1038/s41586-020-2249-1

Capauto, D., Colantoni, A., Lu, L., Santini, T., Peruzzi, G., Biscarini, S., et al. (2018). A regulatory circuitry between Gria2, miR-409, and miR-495 is affected by ALS FUS mutation in ESC-derived motor neurons. *Mol. Neurobiol.* 55 (10), 7635–7651. doi:10.1007/s12035-018-0884-4

Carrieri, C., Cimatti, L., Biagioli, M., Beugnet, A., Zucchelli, S., Fedele, S., et al. (2012). Long non-coding antisense RNA controls Uchl1 translation through an embedded SINEB2 repeat. *Nature* 491 (7424), 454–457. doi:10.1038/nature11508

Carvelli, A., Setti, A., Desideri, F., Galfrè, S. G., Biscarini, S., Santini, T., et al. (2022). A multifunctional locus controls motor neuron differentiation through short and long noncoding RNAs. *EMBO J.* 41 (13), e108918. doi:10.15252/embj.2021108918

Cipriano, A., and Ballarino, M. (2018). The ever-evolving concept of the gene: The use of RNA/protein experimental techniques to understand genome functions. *Front. Mol. Biosci.* 5 (20). doi:10.3389/fmolb.2018.00020

D'Ambra, E., Santini, T., Vitiello, E., D'Uva, S., Silenzi, V., Morlando, M., et al. (2021). Circ-Hdgfrp3 shuttles along neurites and is trapped in aggregates formed by ALS-associated mutant FUS. *iScience* 24 (12), 103504. doi:10.1016/j.isci.2021.103504

Desideri, F., Cipriano, A., Petrezselyova, S., Buonaiuto, G., Santini, T., Kasparek, P., et al. (2020). Intronic determinants coordinate charme lncRNA nuclear activity through the interaction with MATR3 and PTBP1. *Cell Rep.* 33 (12), 108548. doi:10.1016/j.celrep.2020.108548

Engreitz, J. M., Sirokman, K., McDonel, P., Shishkin, A. A., Surka, C., Russell, P., et al. (2014). RNA-RNA interactions enable specific targeting of noncoding RNAs to nascent Pre-mRNAs and chromatin sites. *Cell* 159 (1), 188–199. doi:10.1016/j.cell.2014.08.018

Fatica, A., and Bozzoni, I. (2014). Long non-coding RNAs: New players in cell differentiation and development. *Nat. Rev. Genet.* 15 (1), 7–21. doi:10.1038/nrg3606

Fatima, R., Akhade, V. S., Pal, D., and Rao, S. M. (2015). Long noncoding RNAs in development and cancer: Potential biomarkers and therapeutic targets. *Mol. Cell. Ther.* 3, 5. doi:10.1186/s40591-015-0042-6

Ferrè, F., Colantoni, A., and Helmer-Citterich, M. (2016). Revealing protein-lncRNA interaction. *Brief. Bioinform.* 1, 106–116. doi:10.1093/bib/bbv031

Fukunaga, T., and Hamada, M. (2017). RIblast: An ultrafast RNA-RNA interaction prediction system based on a seed-and-extension approach. *Bioinformatics* 33 (17), 2666–2674. doi:10.1093/bioinformatics/btx287

Fukunaga, T., Iwakiri, J., Ono, Y., and Hamada, M. (2019). LncRRIsearch: A web server for lncRNA-RNA interaction prediction integrated with tissue-specific expression and subcellular localization data. *Front. Genet.* 10, 462. doi:10.3389/fgene.2019.00462

Goff, L. A., Groff, A. F., Sauvageau, M., Trayes-Gibson, Z., Sanchez-Gomez, D. B., Morse, M., et al. (2015). Spatiotemporal expression and transcriptional perturbations by long noncoding RNAs in the mouse brain. *Proc. Natl. Acad. Sci. U. S. A.* 112 (22), 6855–6862. doi:10.1073/pnas.1411263112

Gong, C., and Maquat, L. E. (2011). lncRNAs transactivate STAU1-mediated mRNA decay by duplexing with 3' UTRs via Alu elements. *Nature* 470 (7333), 284–288. doi:10.1038/nature09701

Gong, J., Shao, D., Xu, K., Lu, Z., Lu, Z. J., Yang, Y. T., et al. (2018). RISE: A database of RNA interactome from sequencing experiments. *Nucleic Acids Res.* 46 (D1), D194-D201–D201. doi:10.1093/nar/gkx864

Guil, S., and Esteller, M. (2015). RNA-RNA interactions in gene regulation: The coding and noncoding players. *Trends biochem. Sci.* 40 (5), 248–256. doi:10.1016/j.tibs.2015.03.001

Hafner, M., Katsantoni, M., Köster, T., Marks, J., Mukherjee, J., Staiger, D., et al. (2021). CLIP and complementary methods. *Nat. Rev. Methods Prim.* 1 (1), 20–23. doi:10.1038/s43586-021-00018-1

Hansen, T. B., Jensen, T. I., Clausen, B. H., Bramsen, J. B., Finsen, B., Damgaard, C. K., et al. (2013). Natural RNA circles function as efficient microRNA sponges. *Nature* 495 (7441), 384–388. doi:10.1038/nature11993

Helwak, A., Kudla, G., Dudnakova, T., and Tollervey, D. (2013). Mapping the human miRNA interactome by CLASH reveals frequent noncanonical binding. *Cell* 153 (3), 654–665. doi:10.1016/j.cell.2013.03.043

Herman, A. B., Tsitsipatis, D., and Gorospe, M. (2022). Integrated lncRNA function upon genomic and epigenomic regulation. *Mol. Cell* 82 (12), 2252–2266. doi:10.1016/j.molcel.2022.05.027

Juritsch, A. F., and Moreau, R. (2019). Rapid removal of dextran sulfate sodium from tissue RNA preparations for measurement of inflammation biomarkers. *Anal. Biochem.* 579, 18–24. doi:10.1016/j.ab.2019.05.011

Kerr, T. A., Ciorba, M. A., Matsumoto, H., Davis, V. R., Luo, J., Kennedy, S., et al. (2012). Dextran sodium sulfate inhibition of real-time polymerase chain reaction amplification: A poly-A purification solution. *Inflamm. Bowel Dis.* 18 (2), 344–348. doi:10.1002/ibd.21763

Kopp, F., and Mendell, J. T. (2018). Functional classification and experimental dissection of long noncoding RNAs. *Cell* 172 (3), 393–407. doi:10.1016/j.cell.2018.01.011

Kretz, M., Siprashvili, Z., Chu, C., Webster, D. E., Zehnder, A., Qu, K., et al. (2013). Control of somatic tissue differentiation by the long non-coding RNA TINCR. *Nature* 493 (7431), 231–235. doi:10.1038/nature11661

Kristensen, L. S., Andersen, M. S., Stagsted, L., Ebbesen, K. K., Hansen, T. B., and Kjems, J. (2019). The biogenesis, biology and characterization of circular RNAs. *Nat. Rev. Genet.* 20 (11), 675–691. doi:10.1038/s41576-019-0158-7

Lederman, L. L., Kawasaki, E. S., and Szabo, P. (1981). The rate of nucleic acid annealing to cytological preparations is increased in the presence of dextran sulfate. *Anal. Biochem.* 117 (1), 158–163. doi:10.1016/0003-2697(81)90705-3

Lee, F. C., and Ule, J. (2018). Advances in CLIP technologies for studies of protein-RNA interactions. *Mol. Cell* 69 (3), 354–369. doi:10.1016/j.molcel.2018.01.005

Lekka, E., and Hall, J. (2018). Noncoding RNAs in disease. *FEBS Lett.* 592 (17), 2884–2900. doi:10.1002/1873-3468.13182

Lerner, M. R., and Steitz, J. A. (1979). Antibodies to small nuclear RNAs complexed with proteins are produced by patients with systemic lupus erythematosus. *Proc. Natl. Acad. Sci. U. S. A.* 76 (11), 5495–5499. doi:10.1073/pnas.76.11.5495

Li, L., and Chang, H. Y. (2014). Physiological roles of long noncoding RNAs: Insight from knockout mice. *Trends Cell Biol.* 24 (10), 594–602. doi:10.1016/j.tcb.2014.06.003

Martone, J., Mariani, D., Santini, T., Setti, A., Shamloo, S., Colantoni, A., et al. (2020). SMaRT lncRNA controls translation of a G-quadruplex-containing mRNA antagonizing the DHX36 helicase. *EMBO Rep.* 21 (6), e49942. doi:10.15252/embr.201949942

Matthews, B. (1988). Protein-DNA interaction. No code for recognition. *Nature* 335, 294–295. doi:10.1038/335294a0

McHugh, C. A., Chen, C. K., Chow, A., Surka, C. F., Tran, C., McDonel, P., et al. (2015). The Xist lncRNA interacts directly with SHARP to silence transcription through HDAC3. *Nature* 521 (7551), 232–236. doi:10.1038/nature14443

Moore, M. J. (2005). From birth to death: The complex lives of eukaryotic mRNAs. *Science* 309 (5740), 1514–1518. doi:10.1126/science.1111443

Ni, Y. Q., Xu, H., and Liu, Y. S. (2022). Roles of long non-coding RNAs in the development of aging-related neurodegenerative diseases. *Front. Mol. Neurosci.* 15, 844193. doi:10.3389/fnmol.2022.844193

Phizicky, E. M., and Fields, S. (1995). Protein-protein interactions: Methods for detection and analysis. *Microbiol. Rev.* 59 (1), 94–123. doi:10.1128/mr.59.1.94-123.1995

Piwecka, M., Glažar, P., Hernandez-Miranda, L. R., Memczak, S., Wolf, S. A., Rybak-Wolf, A., et al. (2017). Loss of a mammalian circular RNA locus causes miRNA deregulation and affects brain function. *Science* 357 (6357), eaam8526. doi:10.1126/science.aam8526

Ramanathan, M., Porter, D. F., and Khavari, P. A. (2019). Methods to study RNA–protein interactions. *Nat. Methods* 16, 225–234. doi:10.1038/s41592-019-0330-1

Santini, T., Martone, J., and Ballarino, M. (2021). Visualization of nuclear and cytoplasmic long noncoding RNAs at single-cell level by RNA-FISH. *Methods Mol. Biol.* 2157, 251–280. doi:10.1007/978-1-0716-0664-3_15

Savulescu, A. F., Jacobs, C., Negishi, Y., Davignon, L., and Mhlanga, M. M. (2020). Pinpointing cell identity in time and space. *Front. Mol. Biosci.* 7, 209. doi:10.3389/fmolb.2020.00209

Singer, R. H., and Ward, D. C. (1982). Actin gene expression visualized in chicken muscle tissue culture by using *in situ* hybridization with a biotinated nucleotide analog. *Proc. Natl. Acad. Sci. U. S. A.* 79 (23), 7331–7335. doi:10.1073/pnas.79.23.7331

Singh, L., and Jones, K. W. (1984). The use of heparin as a simple cost-effective means of controlling background in nucleic acid hybridization procedures. *Nucleic Acids Res.* 12 (14), 5627–5638. doi:10.1093/nar/12.14.5627

Statello, L., Guo, C. J., Chen, L. L., and Huarte, M. (2021). Gene regulation by long non-coding RNAs and its biological functions. *Nat. Rev. Mol. Cell Biol.* 22 (2), 96–118. doi:10.1038/s41580-020-00315-9

Ule, J., Jensen, K. B., Ruggiu, M., Mele, A., Ule, A., and Darnell, R. B. (2003). CLIP identifies Nova-regulated RNA networks in the brain. *Science* 302 (5648), 1212–1215. doi:10.1126/science.1090095

Van Gijlswijk, R. P., Wiegant, J., Raap, A. K., and Tanke, H. J. (1996). Improved localization of fluorescent tyramides for fluorescence *in situ* hybridization using dextran sulfate and polyvinyl alcohol. *J. Histochem. Cytochem.* 44 (4), 389–392. doi:10.1177/44.4.8601698

Viennois, E., Chen, F., Laroui, H., Baker, M. T., and Merlin, D. (2013). Dextran sodium sulfate inhibits the activities of both polymerase and reverse transcriptase: Lithium chloride purification, a rapid and efficient technique to purify RNA. *BMC Res. Notes* 6, 360. doi:10.1186/1756-0500-6-360

Wahl, G. M., Stern, M., and Stark, G. R. (1979). Efficient transfer of large DNA fragments from agarose gels to diazobenzyloxymethyl-paper and rapid hybridization by using dextran sulfate. *Proc. Natl. Acad. Sci. U. S. A.* 76 (8), 3683–3687. doi:10.1073/pnas.76.8.3683

Wetmur, J. G. (1975). Acceleration of DNA renaturation rates. *Biopolymers* 14, 2517–2524. doi:10.1002/bip.1975.360141208

Wichterle, H., Lieberam, I., Porter, J. A., and Jessell, T. M. (2002). Directed differentiation of embryonic stem cells into motor neurons. *Cell* 110, 385–397. doi:10.1016/s0092-8674(02)00835-8

Wichterle, H., and Peljto, M. (2008). Differentiation of mouse embryonic stem cells to spinal motor neurons. *Curr. Protoc. Stem Cell Biol.* Chapter 1, Unit 1H.1.1–1H.1.9. doi:10.1002/9780470151808.sc01h01s5

Yao, R. W., Wang, Y., and Chen, L. L. (2019). Cellular functions of long noncoding RNAs. *Nat. Cell Biol.* 21, 542–551. doi:10.1038/s41556-019-0311-8